

Diphoton Background to Higgs Boson Production at the LHC with Soft Gluon Effects

C. Balázs, P. Nadolsky, C. Schmidt, and C.-P. Yuan
Michigan State University, East Lansing, MI 48824, U.S.A.
(April 24, 2000)

The detection and the measurement of the production cross section of a light Higgs boson at the CERN Large Hadron Collider demand the accurate prediction of the background distributions of photon pairs. To improve this theoretical prediction, we present the soft-gluon resummed calculation of the $pp \rightarrow \gamma\gamma X$ cross section, including the exact one loop $gg \rightarrow \gamma\gamma g$ contribution. By incorporating the known fixed order results and the leading terms in the higher order corrections, the resummed cross section provides a reliable prediction for the inclusive diphoton invariant mass and transverse momentum distributions. Given our results, we propose the search for the Higgs boson in the inclusive diphoton mode with a cut on the transverse momentum of the photon pair, without the requirement of an additional tagged jet.

PACS number(s): 12.38.Cy, 13.85.Qk.

hep-ph/9905551, CTEQ-905, MSUHEP-90526

I. INTRODUCTION

The direct search for the Standard Model (SM) Higgs boson at the CERN LEP collider constrains its mass m_H to be greater than $\sqrt{s} - m_Z \sim 108$ GeV [1]. Meanwhile, recent electroweak global fits [2], and the measurements of the W^\pm boson and top quark masses [3] suggest that the SM Higgs mass is lower than about 260 GeV. If m_H is less than twice the Z^0 boson mass, as the electroweak fits hint, then at the CERN Large Hadron Collider (LHC) the most promising detection modes of the SM Higgs boson will be $pp \rightarrow HX \rightarrow \gamma\gamma X$ [4] and the associated production $pp \rightarrow H \text{ jet } X \rightarrow \gamma\gamma \text{ jet } X$ [5]. According to earlier studies, a statistical significance on the order of 5-10 can be reached for both of these signals, actual values depending on luminosity and background estimates. In Ref. [5] it was also found that in order to optimize the significance it is necessary to impose a 30 GeV cut on the transverse momentum of the jet, or equivalently (at NLO precision), on the Q_T of the photon pair. With this cut in place extraction of the signal in the Higgs plus jet mode requires the precise knowledge of both the signal and background distributions in the mid- to high- Q_T region.

The precise determination of signal and background rates of the inclusive diphoton process demands the calculation of the large QCD corrections. Higher order corrections, both to the signal [6] and the background [7], increase the rate significantly, by a factor of about 2. In the case of the background this large increase is mostly due to the fact that the diphoton cross section receives a large contribution from the formally higher order $gg \rightarrow \gamma\gamma$ partonic subprocess, which is of the same order of magnitude as the $q\bar{q} + qg \rightarrow \gamma\gamma X$ subprocesses [8]. Since the lowest order $gg \rightarrow \gamma\gamma$ subprocess proceeds through a box diagram, the calculation of yet higher order corrections to this process is complicated.

A reliable calculation of the transverse momentum distribution of the Higgs boson or the background photon pair also requires the resummation of the potentially large logarithmic contributions of the type $\ln(Q/Q_T)$ (where Q is the invariant mass of the pair), arising as a result of multiple soft-gluon emission. Using the soft-gluon resummation technique, the low- to mid- Q_T region can be predicted, and the resummed calculation can be matched to the fixed order, giving a reliable prediction in the whole Q_T range [8,9]. As an added bonus the resummed cross section also exhibits reduced scale dependence since it includes the most important higher order contributions. It also gives a hint of the size of the yet higher order corrections.

The effects of the multiple soft-gluon radiation on the transverse momentum distribution of Higgs bosons were discussed in a recent paper [9]. In the present work, we analyze the same effects on the transverse momentum of the background photon pair, extending results previously published in Refs. [8,10]. When Q_T is integrated, the resummed calculation of Ref. [8] gives the rates for the $q\bar{q} + qg \rightarrow \gamma\gamma X$ subprocesses at the $\mathcal{O}(\alpha^2\alpha_S)$ precision. That calculation also includes the photon fragmentation contribution, and approximates the $\mathcal{O}(\alpha^2\alpha_S^3)$ $gg + qg \rightarrow \gamma\gamma X$ rate. In this work, we include the exact one loop $\mathcal{O}(\alpha^2\alpha_S^3)$ $gg \rightarrow \gamma\gamma g$ calculation to improve the diphoton background prediction in the high Q_T region. The above fixed order and resummed contributions are implemented in the ResBos [11] Monte Carlo event generator which was used to produce our numerical results.

II. ANALYTICAL RESULTS

The one loop $gg \rightarrow \gamma\gamma g$ amplitude can easily be derived from the one loop five-gluon ($5g$) amplitudes of Ref. [12] for the case when the particles in the loop are

fermions in the fundamental representation, by replacing two of the gluon vertices with photon vertices. Since the $5g$ amplitude is explicitly given in a color-decomposed form, it is possible to replace the $SU(3)$ generators and strong couplings (g_S) of two of the gluons with $U(1)$ generators and the electromagnetic couplings (e) of photons. The final expression for the square of the three-gluon-two-photon ($3g2\gamma$) amplitude is

$$|A(g_1 g_2 \rightarrow g_3 \gamma_4 \gamma_5)|^2 = 8(eQ_i)^4 g_S^6 N_C(N_C^2 - 1) \times \sum_{\text{helicities}} \left| \sum_{\sigma \in \text{COP}_4^{(123)}} A_{5,1}^{[1/2]}(\sigma_1, \sigma_2, \sigma_3, \sigma_4, \sigma_5) \right|^2, \quad (1)$$

where σ_i is shorthand for the 4-momenta and helicities, $\{p_{\sigma_i}, \lambda_{\sigma_i}\}$, of the gluons 1,2,3 and the photons 4,5. The charge of the quarks in the loop is given by Q_i in the units of the charge of the positron, and $N_C = 3$ is the number of colors in QCD. In Eq.(1) $\text{COP}_4^{(123)}$ denotes the subset of permutations of (1,2,3,4) that leave the ordering of (1,2,3) unchanged up to a cyclic permutation

$$\begin{aligned} \sum_{\sigma \in \text{COP}_4^{(123)}} A_{5,1}^{[1/2]}(\sigma_1, \sigma_2, \sigma_3, \sigma_4, \sigma_5) = \\ A_{5,1}^{[1/2]}(1, 2, 3, 4, 5) + A_{5,1}^{[1/2]}(1, 2, 4, 3, 5) + \\ A_{5,1}^{[1/2]}(1, 4, 2, 3, 5) + A_{5,1}^{[1/2]}(4, 1, 2, 3, 5) + \\ A_{5,1}^{[1/2]}(3, 1, 2, 4, 5) + A_{5,1}^{[1/2]}(3, 1, 4, 2, 5) + \\ A_{5,1}^{[1/2]}(3, 4, 1, 2, 5) + A_{5,1}^{[1/2]}(4, 3, 1, 2, 5) + \\ A_{5,1}^{[1/2]}(2, 3, 1, 4, 5) + A_{5,1}^{[1/2]}(2, 3, 4, 1, 5) + \\ A_{5,1}^{[1/2]}(2, 4, 3, 1, 5) + A_{5,1}^{[1/2]}(4, 2, 3, 1, 5). \end{aligned} \quad (2)$$

The partial amplitudes $A_{5,1}^{[1/2]}(1, 2, 3, 4, 5)$ for the various helicities of the external gluons and photons are given in Ref. [12].

The extension of the Collins-Soper-Sterman soft-gluon resummation formalism [13] to diphoton production was discussed in Ref. [10]. We follow that work when calculating the $\mathcal{O}(\alpha_S)$ fixed-order corrections to the $q\bar{q} \rightarrow \gamma\gamma$ subprocess, including the fragmentation contributions, and resumming the contributions of the $q\bar{q} \rightarrow \gamma\gamma g$, $qg \rightarrow \gamma\gamma q$ and $\bar{q}g \rightarrow \gamma\gamma \bar{q}$ subprocesses. In addition, Ref. [10] used an approximate expression for the cross-section of the $gg \rightarrow \gamma\gamma g$ subprocess, that accounted for the emission of soft and/or collinear gluons off the initial gluons, and was valid in the limit of small non-zero Q_T .

Using the exact formula (1) for the matrix element of the $gg \rightarrow \gamma\gamma g$ subprocess, we can now also analyze the high- Q_T region. We match the above fixed-order result with the resummed results of Ref. [10], following the procedure of Ref. [11], to obtain a prediction in the whole range of Q_T . In the resummation of the $gg + qg \rightarrow \gamma\gamma g$ process, we use the $A^{(1)}$ and $A^{(2)}$ coefficients of Ref. [14],

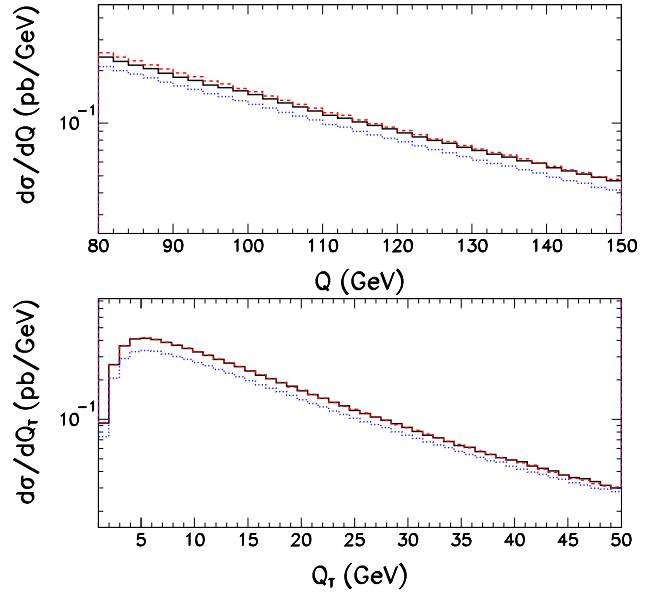


FIG. 1. The resummed part of invariant mass and transverse momentum distributions of photon pairs at the LHC, calculated for the $q\bar{q} + qg \rightarrow \gamma\gamma X$ subprocess using ResBos. The solid curves are calculated using the exact Wilson coefficient $C^{(1)}$. For the dashed curves, $C^{(1)}$ is set identical to that of the Drell-Yan process. For the dotted curves, $C^{(1)}$ is set to zero.

since these coefficients depend only on the initial partons and are independent of the partonic process itself. The $B^{(1)}$ coefficient for the $gg \rightarrow \gamma\gamma g$ process is the same as the one for $gg \rightarrow Hg$, also given in Ref. [14]. The only unknown part of the resummed cross-section for this subprocess is the coefficient $C^{(1)}$, which would require the computation of two-loop virtual diagrams. Following Ref. [10], we approximate $C^{(1)}$ in the process $gg + qg \rightarrow \gamma\gamma g$ by the expression for $C^{(1)}$ in the process $gg \rightarrow Hg$ in the limit of a large top quark mass. This approximation is reasonable when both photons have large transverse momenta, because then the real and virtual corrections are dominated by soft and collinear radiation off external lines, which is identical to that in the Higgs production process.

To support this statement, we examine the behavior of the analogous approximation for the case of the $q\bar{q}, qg, \bar{q}g \rightarrow \gamma\gamma X$ process. We calculate the resummed part of this cross section in three different ways: with an exact $C^{(1)}$, with an approximate $C^{(1)}$, and without the $C^{(1)}$ coefficient. The approximate $C^{(1)}$ coefficient is identical to that of the Drell-Yan process, and omits terms coming from the additional virtual corrections to the hard process (c.f. Eqs. (8) and (11) of [10]). The results are displayed in Fig. 1. The figure shows that the approximation (dashed curve) is better toward the high invariant mass region, which is expected, since Q is correlated with the transverse momentum of the indi-

vidual photon in the central rapidity region. According to the invariance mass plot, the approximation slightly overestimates the rate for low Q 's (by a few percent), and the (dotted) curve without $C^{(1)}$ deviates from the exact (solid) curve by about 20 percent, which is the size of the NLO corrections to this process. In conclusion, the approximate $C^{(1)}$ coefficient (borrowed from the Drell-Yan process) captures most of the NLO corrections for the $q\bar{q}, qg, \bar{q}g \rightarrow \gamma\gamma X$ process, and is a good ansatz for both Q and Q_T , when compared with the exact calculation. In the absence of the exact calculation for the $C^{(1)}$ coefficient, which requires the knowledge of the exact two loop virtual corrections to the $gg + qg \rightarrow \gamma\gamma$ process, we propose to use the approximate $C^{(1)}$ coefficient, borrowed from the $gg \rightarrow HX$ process, to estimate the effect of the higher order corrections to the distributions of the photon pairs. We expect that this should give a better estimate of the event rates than using only the $C^{(0)}$ coefficient in our calculation.

Finally, the small qg component is still approximated as in Ref. [10], noting that it is highly suppressed due to the large difference between the gluon and quark luminosities in the probed region of momentum fraction.

III. NUMERICAL RESULTS

The above described analytic results are implemented in the ResBos Monte Carlo event generator [11]. In the numerical calculations we use the center-of-mass energy 14 TeV and the following electroweak parameters [15]:

$$G_F = 1.16639 \times 10^{-5} \text{ GeV}^{-2}, \quad m_Z = 91.187 \text{ GeV},$$

$$m_W = 80.41 \text{ GeV}, \quad \alpha(m_Z) = \frac{1}{128.88}.$$

We use the NLO expressions for the running electromagnetic and strong couplings $\alpha(\mu)$ and $\alpha_S(\mu)$, as well as the NLO parton distribution function set CTEQ4M. We set the renormalization scale equal to the factorization scale: $\mu_R = \mu_F = Q$. For the choice of the non-perturbative function of the resummation for the various subprocesses, we follow Ref. [10].

Our kinematic cuts, imposed on the final state photons, reflect the optimal detection capabilities of the ATLAS detector [4]:

- $p_T^\gamma > 25 \text{ GeV}$, for the transverse momentum of each photon,
- $|y^\gamma| < 2.5$, for the rapidity of each photon, and
- $p_T^1/(p_T^1 + p_T^2) < 0.7$, to suppress the fragmentation contribution, where p_T^1 is the transverse momentum of the photon with the higher p_T value.

Additionally, we restrict the invariant mass of the photon pair in the relevant region for the light Higgs production:

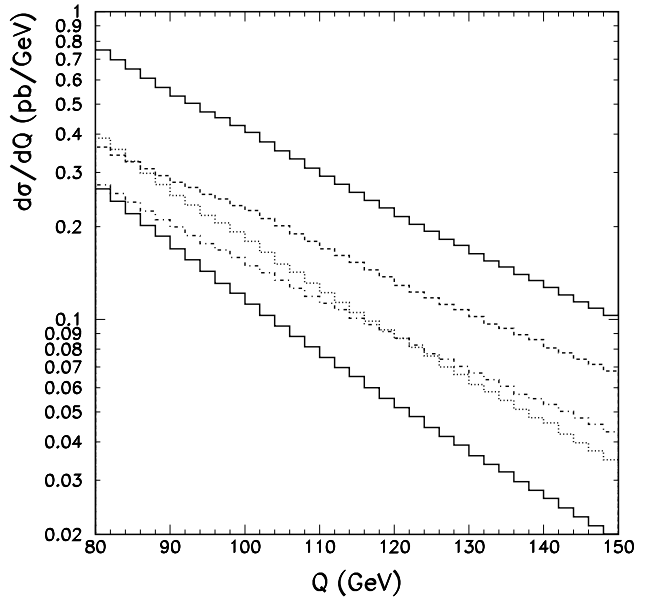


FIG. 2. Invariant mass distributions of photon pairs at the LHC, calculated using ResBos. The total curve (upper solid) is the sum of the $\mathcal{O}(\alpha_S)$ $q\bar{q} + qg \rightarrow \gamma\gamma X$ (dashed) and the $\mathcal{O}(\alpha_S^3)$ $gg + qg \rightarrow \gamma\gamma X$ (dotted) contributions. The leading order curves for the contributions from $\mathcal{O}(\alpha_S^0)$ $q\bar{q} \rightarrow \gamma\gamma$ (dash-dotted) and $\mathcal{O}(\alpha_S^2)$ $gg \rightarrow \gamma\gamma$ (lower solid) are also shown for comparison.

$80 \text{ GeV} < Q < 150 \text{ GeV}$. We also apply a $\Delta R = 0.4$ separation cut on the photons, but our results are insensitive to this cut (cf. Ref. [10]).

In Fig. 2 we display the invariant mass distribution of photon pairs at the LHC in the inclusive process $pp \rightarrow \gamma\gamma X$, calculated using ResBos with the above cuts. We present separately the resummed contribution from the subprocesses $\mathcal{O}(\alpha_S)$ $q\bar{q} + qg \rightarrow \gamma\gamma X$ (dashed) which includes the fragmentation, and $\mathcal{O}(\alpha_S^3)$ $gg + qg \rightarrow \gamma\gamma X$ (dotted), as well as the total distribution (upper solid), which is the sum of these two curves. We also display, for comparison, the leading order contributions from the subprocesses $\mathcal{O}(\alpha_S^0)$ $q\bar{q} \rightarrow \gamma\gamma$ (dash-dotted) and $\mathcal{O}(\alpha_S^2)$ $gg \rightarrow \gamma\gamma$ (lower solid).

The normalization of the resummed cross-section is determined order-by-order by the coefficients $C^{(n)}$, with the coefficient $C^{(1)}$ derived from the NLO corrections. In Fig. 2 we used the exact $C^{(1)}$ for the subprocess $q\bar{q} + qg \rightarrow \gamma\gamma X$, for which the complete NLO cross-section is known. For the subprocess $gg + qg \rightarrow \gamma\gamma X$, in which the NLO virtual corrections have not yet been calculated, we used the approximate $C^{(1)}$ as described in the previous Section. We found that the $\mathcal{O}(\alpha_S^3)$ cross-section is sensitive to $C^{(1)}$. Namely, the resummed cross-section with the approximate $C^{(1)}$ included is about 1.9 times larger than the one with $C^{(1)} = 0$.

In the $Q > 85 \text{ GeV}$ region the contribution of the $q\bar{q} +$

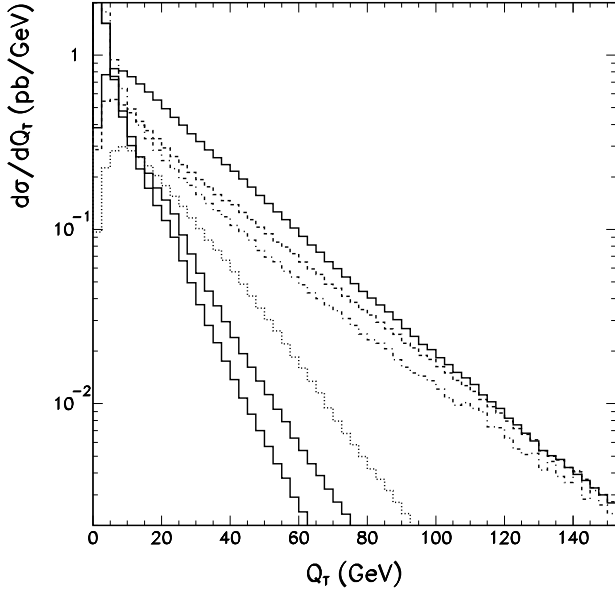


FIG. 3. Transverse momentum distributions of photon pairs at the LHC. The total resummed curve (upper solid) is the sum of the resummed $q\bar{q} + qq \rightarrow \gamma\gamma X$ (dashed), and the resummed $gg + qq \rightarrow \gamma\gamma X$ (dotted) contributions. The fixed-order curves for the contributions from $\mathcal{O}(\alpha_S)$ $q\bar{q} + qq \rightarrow \gamma\gamma X$ (dash-dotted) and $\mathcal{O}(\alpha_S^3)$ $gg + qq \rightarrow \gamma\gamma X$ (middle solid) are also shown for comparison. The approximation for the latter used in [10] is also shown (lower solid).

$gg \rightarrow \gamma\gamma X$ subprocess is higher than that of the $gg + qq \rightarrow \gamma\gamma X$. From Fig. 2 we can also read the K -factors, which are defined as the ratios of the resummed to the leading order results. The K -factor for the $q\bar{q} + qq \rightarrow \gamma\gamma X$ process (the ratio of the dashed and dash-dotted curves) is between 1.40 and 1.70 in the invariant mass range of interest. Similarly, the $gg + qq \rightarrow \gamma\gamma X$ K -factor (the ratio of the dotted and lower solid curves) is between 1.45 and 1.75. This results in an overall K -factor of 1.4 to 1.7. These K -factors are about the same as the NLO/LO K -factors in the fixed order perturbative calculations [6,7].

In Fig. 3 we plot the transverse momentum distribution of photon pairs at the LHC. In addition to the total resummed result, we give the resummed and fixed-order calculations separately for both the $\mathcal{O}(\alpha_S)$ $q\bar{q} + qq \rightarrow \gamma\gamma X$ and the $\mathcal{O}(\alpha_S^3)$ $gg + qq \rightarrow \gamma\gamma X$ subprocesses. In both cases the resummed results deviate substantially from the fixed order predictions in the $0 < Q_T < 100$ GeV region. At $Q_T = 30$ GeV the resummed curves are higher by about 30 and 50 percent for the $q\bar{q} + qq \rightarrow \gamma\gamma X$ and $gg + qq \rightarrow \gamma\gamma X$ subprocesses, respectively. As a result the total resummed curve exceeds the total fixed-order prediction by almost 40 percent at $Q_T = 30$ GeV. This is the Q_T region where the kinematic cuts are applied in order to optimize the statistical significance of the signal in the Higgs plus jet mode. Thus, the use of

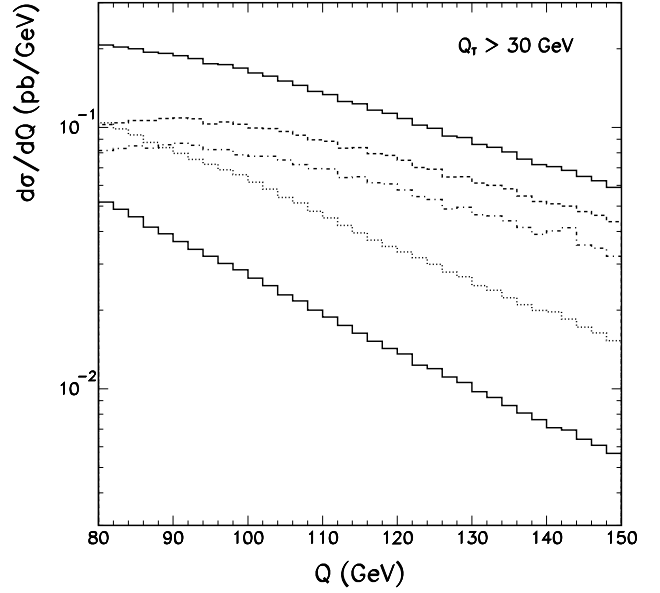


FIG. 4. Invariant mass distributions of photon pairs at the LHC, with the cut $Q_T > 30$ GeV. The total resummed curve (upper solid) is the sum of the resummed $q\bar{q} + qq \rightarrow \gamma\gamma X$ (dashed), and the resummed $gg + qq \rightarrow \gamma\gamma X$ (dotted) contributions. The fixed-order curves for the contributions from $\mathcal{O}(\alpha_S)$ $q\bar{q} + qq \rightarrow \gamma\gamma X$ (dash-dotted) and $\mathcal{O}(\alpha_S^3)$ $gg + qq \rightarrow \gamma\gamma X$ (lower solid) are also shown for comparison.

the resummed prediction is necessary to extract a reliable statistical significance, and also to make a correct determination of the Higgs production cross section, in the presence of kinematic cuts.

Fig. 3 also shows that if the photon pair is constrained to be in the mid- to high- Q_T region the contribution of the $gg + qq \rightarrow \gamma\gamma X$ subprocess is small. At $Q_T = 40$ GeV, for example, the gg initial state accounts for less than 30 percent of the total cross section. In the ResBos program, the $gg + qq \rightarrow \gamma\gamma X$ rate is predicted purely by the resummed calculation and does not cross over into the fixed-order $\mathcal{O}(\alpha_S^3)$ calculation until after about $Q_T = 100$ GeV, at which point this rate is negligible. For reference we also show the approximate fixed order curve used in [10]. The curve calculated using the exact matrix element significantly exceeds the approximation in the high Q_T region.

To illustrate the higher order effects on the invariant mass distribution in the presence of a Q_T cut, in Fig. 4 we plot Q of the photon pair while restricting $Q_T > 30$ GeV. Due to the different shape of the Q_T distributions the cut offsets the fixed-order and resummed rates, as explained in Ref. [11]. The effect is larger for the gg channel, since there the resummed and fixed-order Q_T distributions deviate more, signaling higher corrections to the gg process than to the $q\bar{q}$ process. In the presence of kinematic cuts the difference in the Q distribution,

between the fixed order and the resummed calculations, can be as high as 50 percent. The $Q_T > 30$ GeV cut also suppresses the gg channel, decreasing the uncertainty of the total prediction.

IV. CONCLUSIONS

In this paper we present the resummed calculation of the $pp \rightarrow \gamma\gamma X$ distributions including the exact fixed order $gg \rightarrow \gamma\gamma g$ contribution. Combining the known fixed order QCD corrections and the most important logarithmic terms of the higher order corrections, the resummed cross section provides a reliable prediction for the inclusive diphoton invariant mass and transverse momentum (Q_T) distributions. With a Q_T cut the least reliable $gg \rightarrow \gamma\gamma X$ component can be suppressed, and the prediction further improved.

Given our results, we propose the search for the Higgs boson in the inclusive diphoton mode with a cut on the transverse momentum of the photon pair. This measurement can be done without the requirement of a tagged jet, which is necessary in the $\gamma\gamma$ jet mode. Therefore, it is independent of the jet algorithm used, it can be performed more precisely experimentally, and it can be predicted more reliably from a resummed calculation such as presented here.

While finishing this paper we became aware of a similar work, in which the authors extract the $3g2\gamma$ amplitude from the $5g$ amplitude [16]. Our fixed order analytical and numerical results agree with the results of that paper.

ACKNOWLEDGMENTS

We thank the CTEQ Collaboration, L. Dixon and S. Mrenna for invaluable discussions, J. Huston and M. Abolins for help with the ATLAS parameters and for useful conversations. This work was supported in part by the NSF under grants PHY-9802564 and PHY-9722144.

-
- [1] E. Ferrer, talk given at XXXV Rencontres de Moriond - Elec-troweak and Unified Theories, March 14, 2000; http://moriond.in2p3.fr/EW/2000/transparencies/3_Tuesday/am/Ferrer/
- [2] J. Erler and P. Langacker, hep-ph/9809352; G. D'Agostini and G. Degraffi, hep-ph/9902226; J. Erler, hep-ph/9904235; P. Langacker, hep-ph/9905428.
- [3] B. Abbott *et al.* (D0 Collaboration), Phys. Rev. Lett. **80**, 3008 (1998); B. Abbott *et al.* (D0 Collaboration), hep-ex/9808029; F. Abe *et al.* (CDF Collaboration), Phys. Rev. Lett. **82**, 271 (1999); W.M. Yao (CDF Collaboration), hep-ex/9903068; Y.K. Kim (CDF Collaboration), talk given at *QCD and Weak Boson Physics Workshop*, Fermilab, March 4-6, 1999, <http://cdfsg6.lbl.gov/~ykkim/wmass/lathuile.ps>.
- [4] ATLAS Collaboration, Technical Proposal, CERN/LHC/94-43 LHCC/P2 (1994); CMS Collaboration, Technical Proposal, CERN/LHC/94-43 LHCC/P1 (1994); CMS Collaboration, Technical Design report, CERN/LHCC/97-33 (1997).
- [5] S. Abdullin, M. Dubinin, V. Ilyin, D. Kovalenko, V. Savrin, N. Stepanov, Phys. Lett. **B431**, 410 (1998).
- [6] A. Djouadi, M. Spira and P.M. Zerwas, Phys. Lett. **B 264**, 440 (1991); S. Dawson, Nucl. Phys. **B 359**, 283 (1991); D. Graudenz, M. Spira and P.M. Zerwas, Phys. Rev. Lett. **70**, 1372 (1993); M. Spira, A. Djouadi, D. Graudenz and P.M. Zerwas, Phys. Lett. **B 318**, 347 (1993); R.P. Kauffman and W. Schaffer, Phys. Rev. **D 49**, 551 (1994); S. Dawson and R.P. Kauffman, Phys. Rev. **D 49**, 2298 (1994); M. Spira, A. Djouadi, D. Graudenz and P.M. Zerwas, Nucl. Phys. **B 453**, 17 (1995).
- [7] E.L. Berger, E. Braaten, R.D. Field, Nucl. Phys. **B 239**, 52 (1984); P. Aurenche, A. Douiri, R. Baier, M. Fontannaz, D. Schiff, Z. Phys **C29**, 459 (1985); B. Bailey, J.F. Owens and J. Ohnemus, Phys. Rev. **D 46**, 2018 (1992).
- [8] C. Balázs and C.-P. Yuan, Phys. Rev. **D59**, 114007 (1999).
- [9] C. Balázs and C.-P. Yuan, Phys. Lett. **B478**, 192 (2000) [hep-ph/0001103].
- [10] C. Balázs, E.L. Berger, S. Mrenna and C.-P. Yuan, Phys. Rev. **D57**, 6934 (1998).
- [11] C. Balázs and C.-P. Yuan, Phys. Rev. **D56**, 5558 (1997).
- [12] Z. Bern, L. Dixon, D. Kosower, Phys. Rev. Lett. **70**, 2677 (1993).
- [13] J.C. Collins, D. Soper, Nucl. Phys. **B193**, 381 (1981); Nucl. Phys. **B213**, 545(E) (1983); Nucl. Phys. **B197**, 446 (1982); J.C. Collins, D. Soper, G. Sterman Phys. Lett. **B109**, 388 (1982); Nucl. Phys. **B223**, 381 (1983); Phys. Lett. **B126**, 275 (1983); J.C. Collins, D. Soper, G. Sterman, Nucl. Phys. **B250**, 199 (1985).
- [14] C.-P. Yuan, Phys. Lett. **B283**, 395 (1992); R.P. Kauffman, Phys. Rev. **D45**, 1512 (1992).
- [15] Particle Data Group (C. Caso *et al.*), "Review of Particle Physics", *The European Physical Journal C* **3**, 1 (1998).
- [16] D. de Florian, Z. Kunszt, preprint ETH-TH-99-15, hep-ph/9905283.